A Model-Based Approach to the Automatic Diagnosis of Von Willebrand Disease

Federico Galvanin and Massimiliano Barolo
CAPE-Lab – Computer-Aided Process Engineering Laboratory, Dept. of Industrial Engineering, University of Padova, 35131 Padova, Italy

Roberto Padrini
Dept. of Medicine, University of Padova Medical School, 35128 Padova, Italy

Alessandra Casonato
Dept. of Cardiologic, Thoracic and Vascular Sciences, University of Padova Medical School, 35128 Padova, Italy

Fabrizio Bezzo
CAPE-Lab – Computer-Aided Process Engineering Laboratory, Dept. of Industrial Engineering, University of Padova, 35131 Padova, Italy

DOI 10.1002/aic.14373
Published online February 18, 2014 in Wiley Online Library (wileyonlinelibrary.com)

Von Willebrand disease (VWD) is the most common inherited coagulation disorder to be seen in humans. It originates from a deficiency and/or dysfunction of the von Willebrand factor (VWF), a large multimeric glycoprotein playing a central role in the hemostasis process. VWD occurs in a large variety of forms, and its symptoms may range from sporadic nosebleeds and mild bleeding from small lesions in skin, to acute thrombocytopenia or prolonged bleeding episodes. Diagnosing VWD may be complicated because of the heterogeneous nature of the disorder. Two mechanistic models of VWD are proposed in this article, and their performance is assessed using clinical data. Models allow for the automatic detection of the disease, as well as for a quantitative assessment of VWF multimer distribution patterns, thus elucidating the critical pathways involved in the disease recognition and characterization. © 2014 American Institute of Chemical Engineers *AIChE J*, 60: 1718–1727, 2014
Keywords: Von Willebrand disease, parameter estimation, system identification, clinical data

Introduction

Von Willebrand disease (VWD) is the most common inherited coagulation disorder described in humans. The disease is characterized by a deficiency and/or dysfunction of the von Willebrand factor (VWF), a large multimeric glycoprotein mediating the adhesion and aggregation of platelets to the subendothelium and carrying the coagulation factor VIII (FVIII) in the blood circulation. The predominant clinical symptoms of VWD include nosebleeds, bleeding from small lesions in skin, mucosa, or the gastrointestinal tract, menorrhagia, and excessive bleeding after traumas, surgical interventions, or childbirth.[1] Based on studies performed in Italy and the USA, the most frequently quoted estimate of prevalence of VWD is around 1% .[2,3] More recent data from tertiary health hospitals confirm that based on a population of 5.8 billion, there should be at least 580,000 persons with symptomatic VWD worldwide (100 cases per million persons) and approximately 80% of these persons live in the emerging countries.[4]

Figure 1 shows a sketch of the base mechanisms involved in the distribution of VWF in the bloodstream. VWF is synthesized at the level of endothelial cells and megakaryocytes[5] and then secreted into the plasma. While still in the cells, the VWF subunits form ultralarge (UL) multimers, later cleaved by a specific enzyme (ADAMTS13) in the circulation leading to a precise plasma multimer pattern. VWF is characterized by a complex multimeric structure, with oligomers ranging from 500k to more than 20M daltons, and the largest multimers are the most active hemostatically.[6] Once in the bloodstream, VWF multimers are cleared with a half-life of 12–20 h by a mechanism that is believed not to depend strongly on multimer size.[7] Mean plasma VWF concentrations depend on the balance between the release of VWF from endothelial cells and its removal from the blood circulation, but the extent of modification of multimer distribution, reflecting the competition between clearance and cleavage (proteolysis) by means of ADAMTS13, influences the hemostatic activity of the subject affected by VWD.

VWD is a very heterogeneous disease characterized by a strong intersubject and intrasubject variability. There are three types of VWD (Type 1, Type 2, and Type 3).[8] Type 1 is the most common VWD type, accounting for the 60% of all cases, and depends on a reduction in VWF concentration and on an homogeneous decline in VWF function without important structural anomalies on VWF. Type 2 group includes VWF anomalies with a prevalent functional defect, with four main subtypes, namely 2A, 2B, 2M, and 2N; Type 3 coincides with

Correspondence concerning this article should be addressed to F. Galvanin at federico.galvanin@unipd.it or F. Bezzo at fabrizio.bezzo@unipd.it.

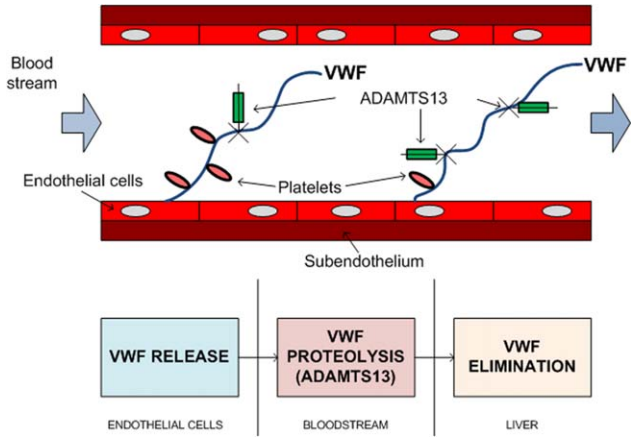

Figure 1. Base mechanisms involved in the distribution of VWF in the bloodstream.

[Color figure can be viewed in the online issue, which is available at wileyonlinelibrary.com.]

the virtual absence of VWF.[1] The exact collocation of subtype Vicenza, a VWD variant characterized by a drastically reduced VWF survival frequently quoted among Type 1, is still a matter of debate in the scientific community.[9]

In the clinical practice, the diagnosis of VWD[8] strongly relies on the clinician's expertise and usually requires a long and time-consuming procedure articulated in distinct phases and levels of investigation. After an initial evaluation of the patient history and a general physical examination, a laboratory diagnosis and monitoring procedure usually starts with a set of initial tests carried out *in vivo* for the detection of VWD by analyzing VWF levels. Preliminary tests for VWD screening involve the measurement of the global amount of VWF protein present in plasma (VWF:Ag), the function of the VWF protein that is present as ristocetin cofactor activity (VWF:RCo) and VWF collagen binding capacity (VWF:CB), and the ability of the VWF to serve as the carrier to factor VIII (FVIII). If one or more of the tests are abnormal, advanced clinical tests (platelet VWF content and VWF multimer count) are required in order to discriminate among possible VWD forms and types. Repetitions of preliminary and advanced diagnostic tests are very frequent, particularly when very low VWF levels are involved in the investigation, because of the poor reproducibility of the clinical tests and the significant intersubject variability.

The availability of a reliable model describing the physiological behavior of a subject suffering from VWD would be beneficial for several reasons: to elucidate the critical pathways involved in the diseases, to optimally design new clinical tests that are shorter, more effective and less stressing for the patient, and possibly to set up more tailored therapeutic approaches.

Single-compartment pharmacokinetic (PK) models allow analyzing the results obtained from PK experiments where VWF plasma concentrations are measured after the subcutaneous administration of a vasopressin analog (DDAVP), forcing the release of VWF from endothelial cells.[10] PK models provide useful indications in the characterization of VWD types by mean of PK indices (elimination half-lives, clearance rates, and amount of DDAVP-induced VWF released). The approach allows for the investigation of several factors affecting VWF survival in the blood stream, including the ABO determinants,[11] VWF clearance rates observed in subtype Vicenza VWD[9] and the VWF functional activity observed in Type 2B VWD.[12] However, the description of a subject's behavior by simple semimechanistic models does not cover the large variety of VWD types and the very high intersubject variability observed during the hemostatic laboratory experimentation.[9,11,12] More importantly, these semimechanistic models do not allow for the description of the real complex physiological patterns involved on VWF multimer time distribution. Although some preliminary modeling efforts have been carried out for understanding the complex interplay of VWF synthesis, clearance, and proteolysis,[13] the proposed models are still based on semimechanistic assumptions, and their performance on prediction strongly relies on the values of the parameters used for describing the initial multimer size distribution. Thus, despite the fact that a quantitative representation of VWF distribution in the blood is required for describing the large variety and forms of the disease encountered in the clinical practice, a reliable mechanistic model for VWD is still missing.

In this article, two new physiologically-based PK models for the description of VWD are presented, allowing for a detailed and quantitative description of the metabolic pathways involved in the disease characterization. The availability of clinical data from PK experiments related to single subjects affected by VWD permits the model identification and the detection of the key physiological responses related to specific variants of the disease, elucidating some complex metabolic mechanisms involved in VWF survival and distribution in the blood stream.

Diagnosis of VWD

VWD diagnosis is the result of a complex procedure where the crucial role of the clinician is to analyze the history of a subject (signs and symptoms of the disease) as well as the amount of quantitative data provided by clinical tests. The usual procedure for VWD diagnosis is illustrated in Figure 2. A laboratory analysis starts after the initial evaluation of a subject, focusing on personal episodes of excessive

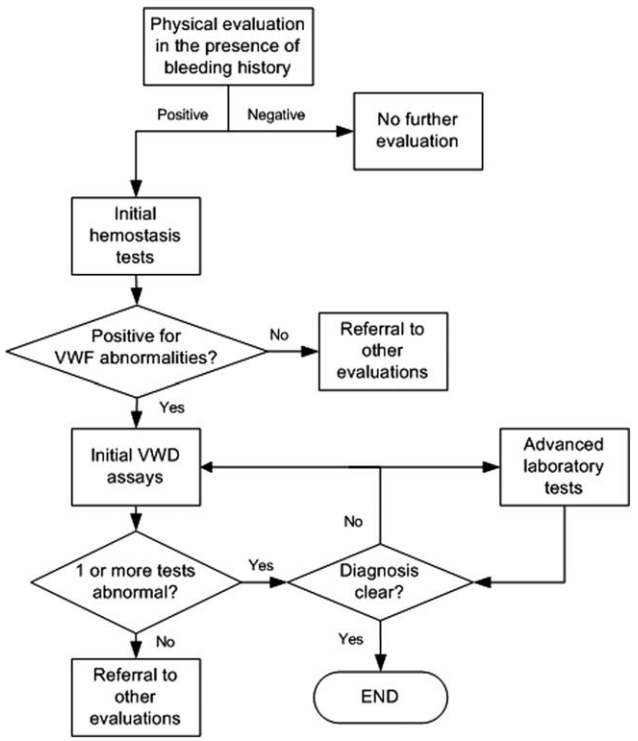

Figure 2. Standard procedure for VWD diagnosis[8].

Table 1. Available Data from Clinical Tests

	Pool of Subjects			
	Healthy		VWD Type	
Measurement Type	O Blood Group	Non-O Blood Group	Vicenza	2B
VWF:Ag/CB	24 subjects	18 subjects	10 subjects	7 subjects
Gel electrophoresis	Average at basal state	Average at basal state	2 subjects	–

bleeding throughout the person's life, and any family history of bleeding disorders, as well as a general physical examination. A preliminary hemostasis laboratory evaluation is then carried out, usually including platelet count, partial thromboplastin time, prothrombin time and, optionally, either fibrinogen or a thrombin time evaluation. If the subject's history evidences a bleeding disorder or abnormal coagulative activity, initial VWD assays can be started including (1) the measurements of the amount of plasma VWF (VWF:Ag); (2) the function of VWF present (VWF:RCo); (3) FVIII.

VWF:Ag gives a quantitative measurement of the global amount of plasma VWF, which is largely independent from the VWF multimer size. VWF:RCo assay measures the ability of VWF to interact with normal platelets. Albeit still largely adopted in the clinical practice, VWF:RCo assay is a time-consuming and not reproducible test with a strong intralaboratory and interlaboratory variability (around 30% or greater if low VWF values are measured).[14] For such reasons, the VWF:RCo has been partially substituted by the VWF collagen-binding (VWF:CB) assay.[15] VWF:CB measures binding of VWF to Type I and III collagen and is dependent on VWF multimeric size, with largest multimers having a greater affinity for the collagen than the smaller forms. The VWF:RCo to VWF:Ag ratio (or the VWF:CB to VWF:Ag ratio) can be useful in the diagnosis of types 2A, 2B, and 2M VWD and help differentiating them from Type 1 VWD.[8] If the aforementioned initial VWD tests are insufficient to provide a precise characterization of VWD and are likely to indicate an impair on coagulative functions, advanced laboratory tests are required, including the analysis of multimer distribution, ristocetin-induced platelet aggregation, the binding of FVIII to VWF (VWF:FVIIIB), or the execution of even more specific (oriented) studies (DDAVP test and DNA sequencing). The VWF multimer test is an advanced test that depicts the variable concentrations of the different sized VWF multimers by using sodium dodecyl sulfate electrophoresis followed by detection of the VWF multimers in the gel. Analysis of gel electrophoresis images offers an essential information on plasma multimer pattern, underlining the relative deficiency of high molecular weight multimers observed in Type 2A and 2B VWD.

Although the combined use of the aforementioned tests is usually sufficient for a precise identification of VWD types, the procedure for achieving a correct diagnosis of VWD is based on a long and very time consuming laboratory activity. Although initial VWD assays are relatively quick and easy to carry out thanks to conventional blood tests readily available in many hospitals, advanced laboratory tests usually require long recovery times for the subjects (even more than 24 h for the DDAVP test) and very specialized laboratories, such that the results of some of these tests may not be available earlier than 2–3 weeks after blood is drawn. Results from clinical tests sometimes may be hard to analyze and interpret from a clinical perspective. Additionally, the presence of false positives, often occurring because of the high subject intervariability, may severely influence the consistency of diagnosis. For this reason, the final evaluation of the disease is largely left to the experience and expertise of the clinician.

A Pharmacokinetic Model of VWD

A reliable PK model of VWD suitable for *in silico* experimentation should have the following features: (1) it should represent the real physiological pathways involved in the time evolution of VWF concentration; (2) its parameters should be easily identifiable from clinical data; (3) it should be sufficiently flexible to be tailored to the specificity of the single subject affected by VWD; (4) it should represent the multimer distribution in time, in order to facilitate the disease recognition.

The model building procedure for the development of a PK model for the description of VWD follows the procedure described by Galvanin et al.[16] First, a preliminary data analysis is carried out where previous knowledge on the system and the available data are used to formulate alternative mechanisms representing reasonable approximations of the physiological behavior of the subject affected by VWD. Candidate models are then formulated, and the available data are used for a preliminary model discrimination using statistical indexes to assess model adequacy.[17] In this study, the commercial software gPROMS[18] is used in each step of the identification procedure.

Preliminary data analysis

Details on the full set of available data are given in Table 1. Clinical data of VWF antigen (VWF:Ag) and collagen binding (VWF:CB) measurements following the subcutaneous administration of DDAVP vasopressin (at a dose of 0.3 μg/kg of body weight) were available for distinct pools of subjects of variable age and body weight including healthy subjects (O and non-O blood group) and subjects affected by VWD (2B and Vicenza). VWF:Ag and VWF:CB measurements were taken during daily tests at fixed times (0, 15, 30, 60, 120, 180, 240, 360, 480, and 1440 min) with a standard deviation on the readings of $\sigma^{Ag} = \sigma^{CB} = 2$ U/dL.

Data from multimeric analysis were available for several subjects affected by the Vicenza type VWD in the form of autoradiographies of VWF multimer pattern obtained from electrophoresis by low resolution agarose gel (1.2%). An example of autoradiography is given in Figure 3a for a subject affected by VWD type Vicenza. Gel electrophoresis is a semiquantitative analysis, and the multimer measurements (collected following the standard protocol at time 0, 30, 60, 120, 180, 240, and 480 min) were obtained by analyzing the optical density (Figure 3b) related to each multimer pattern through image analysis.[19] The average multimer distribution at the basal state (i.e., at the subject's conditions immediately before DDAVP administration) was available for

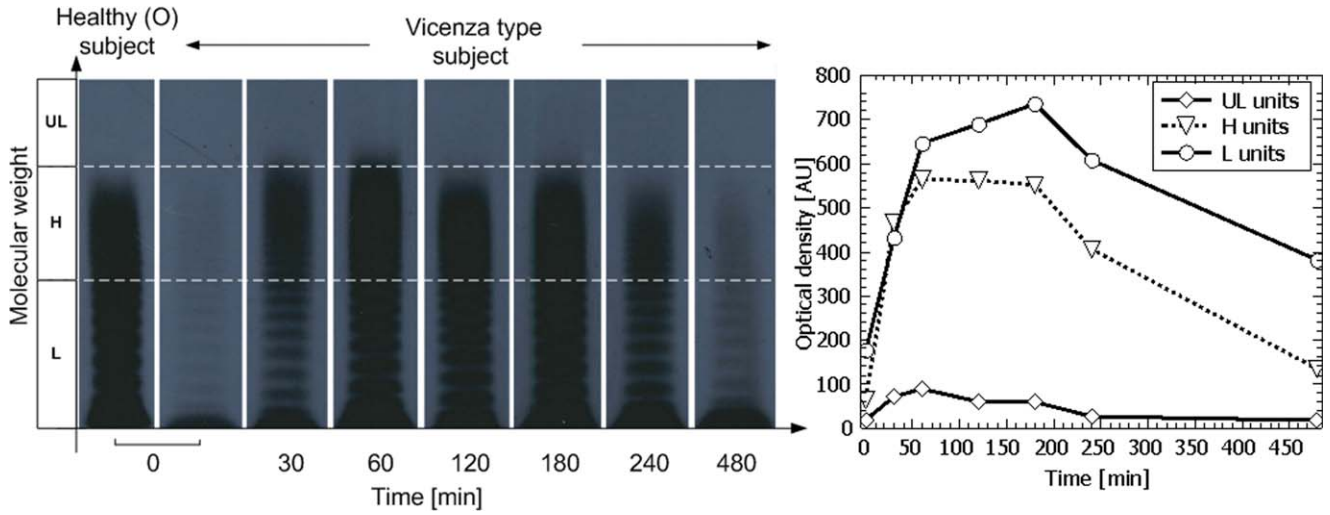

Figure 3. Typical results from a multimeric analysis.

(a) Autoradiography of VWF multimer pattern for a subject affected by VWD type Vicenza; (b) Optical density profiles related to UL, high (H), and low(L) molecular weight multimers obtained from image analysis. [Color figure can be viewed in the online issue, which is available at wileyonlinelibrary.com.]

healthy subjects and provides a baseline for the evaluation of UL, high (H), and low (L) molecular weight multimers in each sample (see Formulation of candidate models section for further details). Measurements are expressed in terms of mass fractions and are available with a standard deviation of $\sigma^{MP} = 0.1$.

Typical average data in terms of VWF:Ag and VWF:CB measurements are illustrated in Figure 4 for healthy (O/non-O) subjects and subjects affected by VWD (Vicenza and 2B types). VWF:Ag measurements (Figure 4a) are related to the global amount of multimers released in plasma, whereas VWF:CB measurements (Figure 4b) quantify the amount of high molecular weight multimers. Healthy subjects exhibit a quantitative similar behavior in terms of VWF:Ag and VWF:CB, characterized by an initial peak (at $\sim$2 h) and a slow VWF concentration decrease until the end of the test. Type 2B subjects show a low amount of high molecular weight multimers (low VWF:CB levels) because of the increased affinity of these multimers for platelet GPIb. Type Vicenza patients are characterized by high clearance rates and low VWF levels without apparent anomalies on multimer size distribution.

Formulation of candidate models

After DDAVP administration, a three-step mechanism is believed to occur[9]:

1. Release of super UL (SUL) multimers; the release rate and amount are subject-dependent;
2. Proteolysis of SUL to smaller species by means of ADAMTS13: SUL multimers are cleaved to UL, high (H), and low (L) molecular weight multimers;
3. Clearance (i.e., multimer elimination from plasma), taking place at the liver level and largely independent of the multimer size.

A preliminary discrimination between rival model structures was carried out using average population data.[16] Eventually, two candidate models were retained: Model 1 and Model 2. Model 1 (Figure 5a) is a compartmental model developed under the following physiological assumptions:

a. At the basal state, only H and L multimers are present;

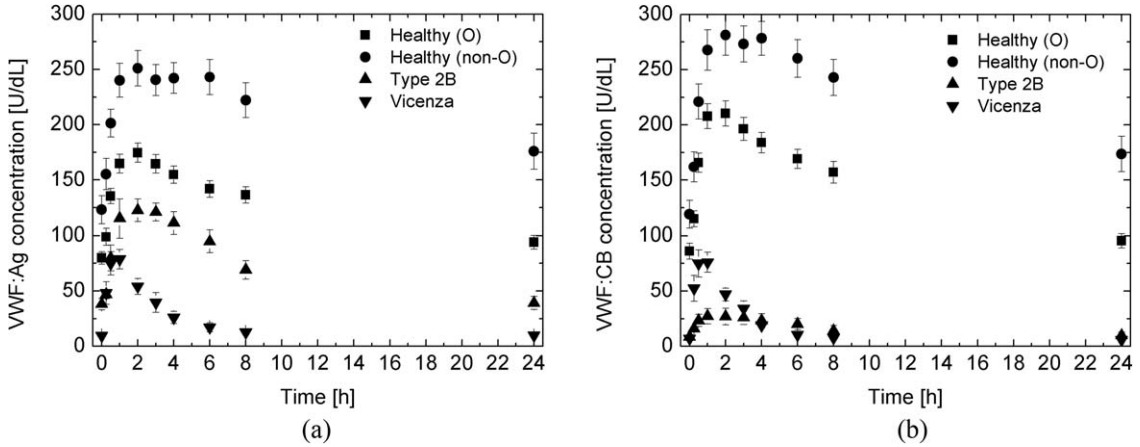

Figure 4. VWF:Ag (a) and VWF:CB (b) average data for normal O subjects (squares), non-O subjects (circles), subjects affected by VWD type 2B (triangles) and Vicenza (reverse triangles).

The error bars represent the variability within the pool in terms of standard deviation.

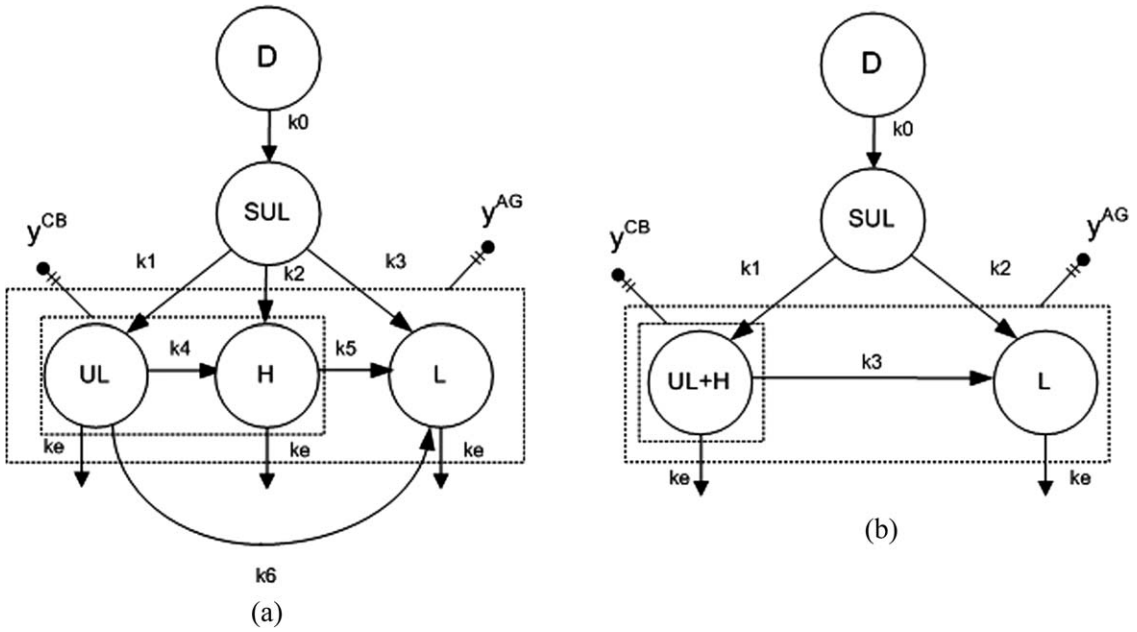

Figure 5. PK model structures considered in this study.

(a) Model 1; (b) Model 2. The location of VWF:Ag and VWF:CB measurements with respect to the compartmental model is indicated by dashed boxes.

b. SUL multimers cannot be measured directly from VWF measurements, and their release (D) is a consequence of DDAVP administration;

c. UL can generate both H and L multimers.

Furthermore, it is assumed that VWF:Ag measurements (y^{AG}) are related to the sum UL+H+L, whereas VWF:CB measurements (y^{CB}) are related to UL+H amount. Data from multimer analysis allow characterizing the amount of UL, H, and L during the clinical trial. A sensitivity-based identifiability analysis showed that Model 1 is characterized by a structural complexity that, because of the poor observability of the UL, H, and L compartments, may lead to identifiability issues if no data from multimeric analysis are available. However, multimeric analysis is time demanding and can be carried out only in properly equipped laboratories. For these reasons, a structurally simplified model (Model 2, Figure 5b) was also developed in order to ensure parameter identifiability when VWF:Ag and VWF:CB data only are available.

Model 1 is described by the following set of differential and algebraic equations

$$\frac{dx^{\mathrm{SUL}}}{dt}=k_0 D\exp^{-k_0(t-t_{\max})}-k_1\left(x^{\mathrm{SUL}}-x_{\mathrm{b}}^{\mathrm{SUL}}\right) -k_2\left(x^{\mathrm{SUL}}-x_{\mathrm{b}}^{\mathrm{SUL}}\right)-k_3\left(x^{\mathrm{SUL}}-x_{\mathrm{b}}^{\mathrm{SUL}}\right)=F_0-F_1-F_2-F_3 \tag{1}$$

$$\frac{dx^{\mathrm{UL}}}{dt}=k_1\left(x^{\mathrm{SUL}}-x_{\mathrm{b}}^{\mathrm{SUL}}\right)-k_4\left(x^{\mathrm{UL}}-x_{\mathrm{b}}^{\mathrm{UL}}\right)-k_{\mathrm{e}}\left(x^{\mathrm{UL}}-x_{\mathrm{b}}^{\mathrm{UL}}\right) -k_6\left(x^{\mathrm{UL}}-x_{\mathrm{b}}^{\mathrm{UL}}\right)=F_1-F_4-F_7-F_6 \tag{2}$$

$$\frac{dx^{\mathrm{H}}}{dt}=k_2\left(x^{\mathrm{SUL}}-x_{\mathrm{b}}^{\mathrm{SUL}}\right)+k_4\left(x^{\mathrm{UL}}-x_{\mathrm{b}}^{\mathrm{UL}}\right)-k_5\left(x^{\mathrm{H}}-x_{\mathrm{b}}^{\mathrm{H}}\right) -k_{\mathrm{e}}\left(x^{\mathrm{H}}-x_{\mathrm{b}}^{\mathrm{H}}\right)=F_2+F_4-F_5-F_8 \tag{3}$$

$$\frac{dx^{\mathrm{L}}}{dt}=k_3\left(x^{\mathrm{SUL}}-x_{\mathrm{b}}^{\mathrm{SUL}}\right)+k_5\left(x^{\mathrm{H}}-x_{\mathrm{b}}^{\mathrm{H}}\right)-k_{\mathrm{e}}\left(x^{\mathrm{L}}-x_{\mathrm{b}}^{\mathrm{L}}\right) +k_6\left(x^{\mathrm{L}}-x_{\mathrm{b}}^{\mathrm{L}}\right)=F_3+F_5+F_6-F_9 \tag{4}$$

where x^{SUL}, x^{UL}, x^{H}, and x^{L} are the number of SUL, UL, H, and L multimer units, respectively, present in the plasma, and subscript "b" is used to define the variables at the basal state.

The F_i terms identify the fluxes between distinct compartments; F_0 represents the release of SUL multimers, which is characterized by k_0 and the release constants D and $t_{\max}$ (here kept fixed to $D=100$ U and $t_{\max}=30$ min, respectively).

In Model 2 (Figure 5b) the sum of UL and H multimer units is modeled by a single compartment described by the following differential equation

$$\frac{dx^{\mathrm{UL+H}}}{dt}=k_1\left(x^{\mathrm{SUL}}-x_{\mathrm{b}}^{\mathrm{SUL}}\right) -k_3\left(x^{\mathrm{UL+H}}-x_{\mathrm{b}}^{\mathrm{UL+H}}\right)-k_{\mathrm{e}}\left(x^{\mathrm{UL+H}}-x_{\mathrm{b}}^{\mathrm{UL+H}}\right) \tag{5}$$

with a significant reduction of the overall number of model parameters to be estimated.

The measured responses are y^{AG} (antigen concentration [U/dL]) and y^{CB} (collagen binding concentration [U/dL])

$$y^{\mathrm{AG}}=\left(x^{\mathrm{UL}}+x^{\mathrm{H}}+x^{\mathrm{L}}\right)/V_d \tag{6}$$

$$y^{\mathrm{CB}}=\left(x^{\mathrm{UL}}+x^{\mathrm{H}}\right)/V_d \tag{7}$$

while multimer measurements allow for the evaluation of the multimer mass fractions in plasma. For each sample (i.e., each dark lane in the autoradiography), the ith multimer mass fraction z_i can be obtained from

$$z_i=x^i/x^T=I^i/I^T=I^i/\sum\nolimits_i I^i \quad i=\mathrm{UL},\ \mathrm{H},\ \mathrm{L} \tag{8}$$

where I^i is the optical density of the ith species, I^{T} is the total optical density, and x^{T} is the total number of multimer units (see Appendix for further details on image analysis). UL-H and H-L limits between multimer species are evaluated from healthy (O) multimer distribution at basal state.

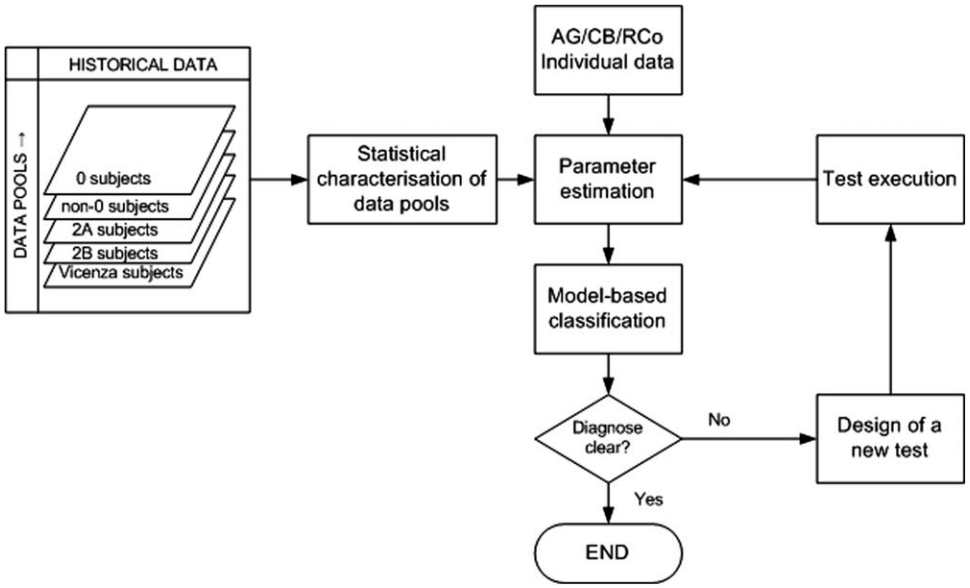

Figure 6. Model-based procedure for VWD diagnosis.

The initial conditions for the integration of the differential system (1–4) are defined by $\mathbf{x}^0 = \mathbf{x}(0) = [\,x_b^{SUL} \quad x_b^{UL} \quad x_b^{H} \quad x_b^{L}\,]^T = [\,0 \quad 0 \quad y_b^{CB} V_d \quad y_b^{AG} V_d - y_b^{CB} V_d\,]^T$; $V_d = 40$ mL/kg body weight is the approximated distribution volume following Ref. 20. A correction is introduced in the definition of the collagen binding measurements in order to account for the different affinity of multimers to collagen observed for distinct VWD types

$$y^{CB'} = k y^{CB} \frac{y_b^{AG}}{y_b^{CB}} = k y^{CB} \left(1 + \frac{x_b^{L}}{x_b^{H}}\right) \tag{9}$$

After a reparameterization in order to guarantee the structural identifiability of the model,[16] the set of parameters to be estimated is $\theta^{M1} = [\,k_0 D/k_e \quad k_1 \quad k_2 \quad k_3 \quad k_4 \quad k_5 \quad k_6 \quad k_e\,]$ for Model 1, and $\theta^{M2} = [\,k_0 D/k_e \quad k_1 \quad k_2 \quad k_3 \quad k_e\,]$ for Model 2, with the additional correction parameters k and y_b^{CB} of (7).

Model-Based Diagnosis of VWD

The model allows for a quantitative description of the VWF levels, and can be used as a support tool for VWD diagnosis. A model-based procedure for the automatic diagnosis of VWD is illustrated in Figure 6. The pathophysiological condition of a subject (healthy O/non-O blood group, Type 2B, and type Vicenza VWD) can be determined by exploiting: (1) the individual measurements including VWF:Ag/VWF:CB data or (possibly) data from multimeric analysis; (2) the VWF:Ag/VWF:CB historical data related to each pool of subjects. For each measured response y, the variability within each available pool of subjects must be characterized in statistical terms by adopting a heteroscedastic variance model in the form

$$\sigma^2 = \omega^2 (y)^{\gamma} \tag{10}$$

where ω and γ are parameters estimated by regression from average data allowing one to build a time-dependent uncertainty region for the model response. Results are given in Table 2.

Given average VWF:Ag/VWF:CB data and the variance model (10), two strategies are possible for the automatic diagnosis of VWD depending on the measurements availability:

1. Strategy S1: diagnosis with Model 1 based on mass fraction measurements from multimeric analysis;
2. Strategy S2: diagnosis with Model 2 from VWF:Ag/CB data.

Under these conditions, both Model 1 and Model 2 are identifiable and the model-based VWD classification is realized by comparing the relative statistics obtained after parameter estimation in terms of sum of squared weighted residuals (SSWR)

$$\mathrm{SSWR} = \sum_{i=1}^{N} \sum_{j=1}^{M} \sum_{k=1}^{N_{sp}} r_{ijk}^2 / \sigma_{ijk}^2 \tag{11}$$

where r_{ijk} is the residual related to the kth sampling point of the jth measured response in the jth experiment with a standard deviation σ_{ijk}, N is the total number of experiments, M is the number of measured responses, and N_{sp} is the number of sampling points per experiment. Average VWF:Ag/CB levels evaluated from the available set of measurements (Table 2) were used to achieve a preliminary estimation of the model parameters for each single class of subjects. These estimates were then used as a starting guess for the identification of the model parameters for single subjects.

Strategy S1: Diagnosis from multimeric analysis

Results in terms of estimated profiles for a subject affected by VWD type Vicenza (Subject A) are given in Figure 7,

Table 2. Parameter Estimation Results for the Variance Model (10)

Response	Param.	O	Non-O	Vicenza	2B
VWF:Ag	ω	0.63	5.51	0.59	0.48
	γ	0.50	0.18	0.66	0.67
VWF:CB	Ω	0.28	2.55	0.24	0.20
	γ	0.69	0.34	0.89	1.08

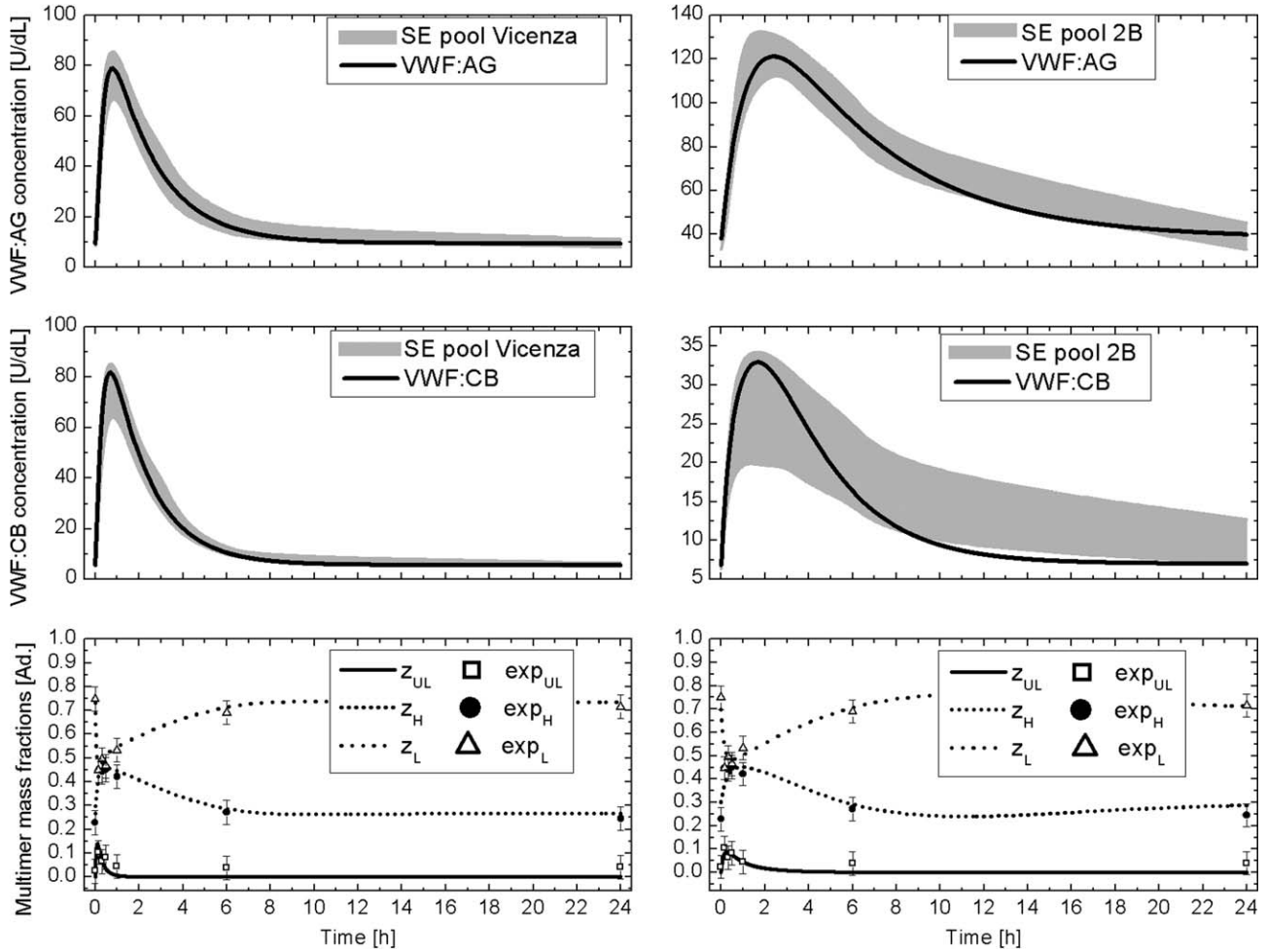

Figure 7. Strategy S1: Subject A. VWF:Ag and VWF:CB profiles and multimer fractions obtained after parameter estimation from multimer measurements associated with the Vicenza (left column) and the 2B (right column) pool of subjects.

The variability within the pool of subjects is indicated by the gray area in terms of standard error.

where the uncertainty of VWF:Ag and VWF:CB measurements associated with the Vicenza and the 2B pool of subjects is indicated by the gray area in terms of standard error. It appears that the association with the 2B pool causes the VWF profiles (right column) to move slightly outside the uncertainty region of the pool. In addition to that, the H and L multimer fractions are evaluated in a less precise way. Even if not shown for the sake of conciseness, a similar behavior is obtained also for subject B. Table 3 confirms that the lowest value of SSWR is achieved when the individual multimer measurements are coupled with the data from the Vicenza pool of subjects. The diagnosis for subject A is, therefore, unambiguous and a good representation of the multimer distribution can also be realized.

The estimated values of Model 1 parameters for subjects A and B affected by VWD type Vicenza are reported in Table 4. The information obtained from the available measurements is sufficient to estimate the full set of parameters in a statistically precise way except k_4 for subject B (for this specific subject, parameter estimation moves the parameter to the assigned lower bound, leading to the elimination of the UL-to-H pathway). Interestingly, some physiological aspects can be remarked. First of all, for both subjects the UL-to-L pathway (parameter k_6) seems to be preferred to cleave UL species to smaller ones. H species are in fact mainly formed by a direct SUL cleavage (k_2) without being cleaved to L (k_5) and eventually eliminated. Second, subject B shows a deficiency on VWF release and a minor reduction

Table 3. Results from Model-Based Diagnosis in Terms of Sum of Squared Weighted Residuals (the Lowest Value is Indicated in Boldface); the VWD Subtype from Medical Evaluation is Indicated for Each Subject Between Parenthesis.

Strategy	Subject	O	Non-O	2B	Vicenza	Model-Based Diagnosis
S1	A (Vicenza)	101	98	23	**9**	**Vicenza**
	B (Vicenza)	267	251	150	**98**	**Vicenza**
S2	C (Vicenza)	107	102	133	**35**	**Vicenza**
	D (Non-O)	1236	**1229**	1958	5083	**Non-O**
	E (Non-O)	5350	**3409**	7268	9148	**Non-O**
	F (2B)	92	87	**20**	177	**2B**

Table 4. Parameter Estimation Results After Model-Based Diagnosis (the Numbers in Boldface Refer to Parameters Failing the 95% t-Test)

		Subject					
Model	θ	A	B	C	D	E	F
Model 1	k^0	0.059	0.024	–	–	–	–
	k^1	0.050	0.036	–	–	–	–
	k^2	0.198	0.046	–	–	–	–
	k^3	0.190	0.001	–	–	–	–
	k^4	0.002	**0.000**	–	–	–	–
	k^5	0.001	0.001	–	–	–	–
	k^6	0.038	0.443	–	–	–	–
	k^e	0.010	0.007	–	–	–	–
Model 2	k^0	–	–	0.051	0.068	0.064	0.055
	k^1	–	–	0.021	0.006	0.006	0.029
	k^2	–	–	0.003	0.001	0.001	0.028
	k^3	–	–	0.001	0.000	0.000	0.003
	k^e	–	–	0.007	0.002	0.001	0.003
Correct. param.	k	0.640	0.580	0.401	1.01	1.13	0.13
	y_b^{CB}	1.87	2.56	2.67	61.99	64.2	5.6

of SUL to L (k_3) if compared to subject A. This highlights the strong intersubject variability that may be encountered even within the same pool of subjects.

Strategy S2: Diagnosis from VWF:Ag and VWF:CB data

Data from multimeric analysis are usually difficult and expensive to obtain, as they require a specific knowledge on the electrophoresis techniques and a significant effort in terms of analytical resources. However, the use of the simplified model (Model 2) allows for a model-based diagnosis simply using individual VWF levels. As shown in Table 3, the use of Model 2 (which uses only VWF:Ag and VWF:CB measurements) provides for an exact diagnosis and generally allows for a clear distinction between the different pathophysiological conditions, except in one case (non-O subject D), where the difference between a O and non-O diagnosis is hardly noticeable, due to the significant intersubject variability in the measurements of VWF levels. Parameter estimation results (Table 4) show that the model parameters are estimated in a statistically sound way for each individual subject. Some physiological aspects can be observed for the different VWD types: (1) the order of magnitude of release parameter k_0 is nearly the same for all the investigated subjects; (2) Vicenza subject C shows an higher elimination rate (k_e) and increased proteolytic activity if compared to healthy non-O subjects (mainly related to SUL decomposition to high molecular weight multimers; k_1); (3) non-O subjects (D and E) show a reduction of proteolysis in the SUL-to-L channel (k_2), and the total absence of the (UL+H)-to-L pathway (k_3); (4) 2B subject F shows an increased proteolytic activity for both SUL-to-L and SUL-to-(UL+H) channels (parameters k_1 and k_2, respectively), and a slight increase on clearance rate if compared to healthy subjects.

Discussion of results

The availability of a physiological model for the description of VWF levels allows for a clear discrimination among subjects and, consequently, can represent a valuable tool for a precise diagnosis of the disease. The proposed models allow for a precise and quantitative description of VWF levels including the characterization of release, proteolysis, and clearance pathways. If advanced laboratory tests, including multimeric analysis data, are available, Model 1 offers a better understanding and a more precise characterization of the proteolysis pathways, describing the multimeric patterns in a more detailed way. A simplified model (Model 2) can be conveniently used if a diagnosis must be carried only simply from VWF levels. In fact, Model 2 may provide a valuable tool for a quick diagnosis from a single set of VWF:Ag and VWF:CB data coming from VWD assays from an individual subject. Additionally, Model 2 gives the potential advantage of making it possible to identify the model parameters if insufficient clinical data are available or if data are affected by large measurements noise.

Final Remarks

Two mechanistic models for the description of VWD have been presented in this article allowing for a physiological interpretation and the quantitative assessment of the biochemical pathways involved in different types of VWD. Models, identified from clinical data, can be used to describe the mechanism of release, distribution, and elimination of VWD from the blood stream for distinct pools of subjects, thanks to the evaluation of the model parameters. The models can be tailored to the specificity of the single subject affected by VWD and allow for a quantitative description of the VWF multimer distribution in time for a faster and more effective diagnosis from clinical data. Additionally, they may represent the basis for a procedure of model-based diagnosis, where data are used to define the unknown pathophysiological condition of a subject. If properly tuned-up and adapted to the specific response of individual subjects, the models can be effectively used to perform *in silico* experiments, suggesting which mechanisms should be investigated for the development of customized therapeutic procedures. Furthermore, the models can be used to design tests which are shorter and easier to implement in the clinical practice, with great benefit in terms of comfort and safety for the subject. Future work will be required to extend the model applicability to other VWD types and to apply the model-

based diagnosis procedure in order to discriminate among possible VWD subtypes.

Acknowledgment

The authors gratefully acknowledge the financial support granted to this work by the University of Padova under Progetto di Ateneo CPDA127585/12 "Towards a mechanistic description of the von Willebrand disease: a process systems engineering approach to model development and design" and Project CPDR110403-2011 on "Optimal design of pharmacodynamic and pharmacokinetic experiments for the identification of physiologically-based models for drug development."

Literature Cited

1. Lillicrap D. Von Willebrand disease—phenotype versus genotype: deficiency versus disease. *Thromb Res*. 2007;120:S11–S16.
2. Rodeghiero F, Castaman G, Dini E. Epidemiological investigation of the prevalence of von Willebrand's disease. *Blood*. 1987;69:454–459.
3. Werner EJ, Broxson EH, Tucker EL, Giroux DS, Shults J, Abshire TC. Prevalence of von Willebrand disease in children: a multiethnic study. *J Pediatr*. 1993;123:893–898.
4. Goodeve AC. The genetic basis of von Willebrand disease. *Blood Rev*. 2010;24:123–134.
5. Sadler JE, Mannucci PM, Berntorp E, Bochkov N, Boulyjenkov V, Ginsburg D, Meyer D, Peake I, Rodeghiero F, Srivastava A. Impact, diagnosis and treatment of von Willebrand disease. *J Thromb Haemost*. 2000;84:160–174.
6. Ruggeri ZM, Pareti FI, Mannucci PM, Ciavarella N, Zimmernal TS. Heightened interaction between platelets and factor VIII/von Willebrand factor in a new subtype of von Willebrand disease. *N Engl J Med*. 1980;302:1047–1051.
7. Lenting PJ, Van Schooten CJM, Denis CV. Clearance mechanisms of von Willebrand factor and factor VIII. *J Thromb Haemost*. 2007; 5:1353–1360.
8. N.H.L.B.I. The diagnosis, evaluation and management of von Willebrand disease. NIH Publication No. 8–5832. U.S. Department of Health and Human Servicies, Bethesda, MD, 2007.
9. Casonato A, Pontara E, Sartorello F, Cattini MG, Sartori MT, Padrini R, Girolami A. Reduced von Willebrand factor survival in type Vicenza von Willebrand disease. *Blood*. 2002;99:180–184.
10. Gezsi A, Balazsi G, Sallai K, Mohl A, Nagy E, Szabo T, Sadler JE, Bodo I. Increased clearance explains the ultra-large multimers in von Willebrand disease type 2M Vicenza; lessons from recombinant VWF Vicenza and modeling of multimer catabolism. *Blood*. 2004; 104:998–1021.
11. Gallinaro L, Cattini MG, Sztukowska M, Padrini R, Sartorello F, Pontara E, Bertomoro A, Daidone V, Pagnan A, Casonato A. A shorter von Willebrand factor survival in O blood group subjects explains how ABO determinants influence plasma von Willebrand factor. *Blood*. 2008;111:3540–3545.
12. Casonato A, Gallinaro L, Cattini MG, Pontara E, Padrini R, Bertomoro A, Daidone V, Pagnan A. Reduced survival of type 2B von Willebrand factor, irrespective of large multimer representation of thrombocytopenia. *Haematologica*. 2010;95:1366–1372.
13. Gezsi A, Budde U, Deak I, Nagy E, Mohl A, Schlammadinger A, Boda Z, Masszi T, Sadler JE, Bodo I. Accelerated clearance alone explains ultra-large multimers on von Willebrand disease Vicenza. *J Thromb Haemost*. 2010;8:1273–1280.
14. Turecek PL, Siekmann J, Schwarz HP. Comparative study on collagen-binding enzyme-linked immunosorbent assay and ristocetin cofactor activity assays for detection of functional activity of von Willebrand factor. *Semin Thromb Hemost*. 2002;28:149–160.
15. Favaloro EJ, Thom J, Patterson D, Just S, Dixon T, Koutts J, Baccala M, Rowell J, Baker R. Desmopressin therapy to assist the functional identification and characterisation of von Willebrand disease: differential utility from combining two (VWF:CB and VWF:RCo) von Willebrand factor activity assays? *Thromb Res*. 2009;123:862–868.
16. Galvanin F, Ballan CC, Barolo M, Bezzo F. A general model-based design of experiments approach to achieve practical identifiability of pharmacokinetic and pharmacodynamic models. *J Pharmacokinet Pharmacodyn*. 2013;40:451–467.
17. Stewart WE, Henson TL, Box GEP. Model discrimination and criticism with single-response data. *AIChE J*. 1996;42:3055–3062.
18. Process Systems Enterprise. gPROMS model validation guide (v. 3.6). London: Process Systems Enterprise, 2012:1–72.
19. Ye X, Suen CY, Cheriet M, Wang E. A recent development in image analysis of electrophoresis gel. Vision Interface '99. Canadian Image Processing and Pattern Recognition Society, Trois-Rivières, Canada, May 19–21, 1999.
20. Menache D, Aronson DL, Darr F, Montgomery RR, Gill JC, Kessler CM, Lusher JM, Phatak PD, Shapiro AD, Thompson AR, White GC. Pharmacokinetics of von Willebrand factor and factor VIIIC in patients with severe von Willebrand disease (type 3 VWD): estimation of the rate of factor VIIIC synthesis. *Br J Haematol*. 1996;94:740–745.

Appendix: Analysis of Gel Electrophoresis Images

The available images from gel electrophoresis show the pattern of multimeric units at fixed times after DDAVP administration. Images (see Figure 3a in the main text) are constituted by:

1. A reference lane, showing the normal distribution of multimers at the basal state for healthy (O) subjects;
2. Seven distinct lanes describing the multimeric pattern for a subjects affected by VWD at 0, 30, 60, 120, 180, 240, 480 min after DDAVP administration.

Each image is analyzed after a pretreatment involving grayscale conversion and background removal, following the procedure described by Ye and coworkers.[19] The size of each single lane is 400 $\times$ 1800 pixels (width (W) $\times$ height (H)) and the pixel intensity values are stored in a ($W \times H$) matrix $\mathbf{i}$ of pixel intensity. The grayscale intensity is stored as an 8-bit integer giving 256 possible levels of gray from black to white. An example of image analysis for a single lane is given in Figure A1. A one-dimensional profile of optical density (Figure A1b) can be defined by evaluating the optical density along the H-direction

$$I_j = \log_2 \left(W \frac{255}{\sum_{k=1}^{W} i_{jk}} \right) j = 1 \ldots H \tag{A1}$$

where i_{jk} is the jkth element of $\mathbf{i}$. According to (A1) the optical density profile is obtained by considering an average value for pixel intensity along the W-direction. The evaluation of UL-H and H-L thresholds (l_1 and l_2) are defined from the reference lane (Figure A1a). In particular, l_1 represents the first pixel position along the H-direction such that $I_j > \varepsilon$, where ε is a small nonzero number related to the noise level of the image (here fixed to 0.05). As at the beginning of the test only H and L are present, l_1 is defined as the pixel position where optical density starts to increase as an effect of the presence of high molecular weight (H) multimers.

The H-L threshold is evaluated from the following expression

$$l_2 = l_1 + \frac{R}{R+1}[H - l_1] \tag{A2}$$

where R represents the VWF:CB/VWF:Ag ratio (according to Gallinaro et al.[11] $R = 1.01$ as evaluated from average data available for healthy O subjects). The evaluation of the area under the curve of the optical density profile for a single sample allows for the definition of the optical densities of the multimeric species

$$I^{\mathrm{UL}} = \int_0^{l_1} Idl \tag{A3}$$

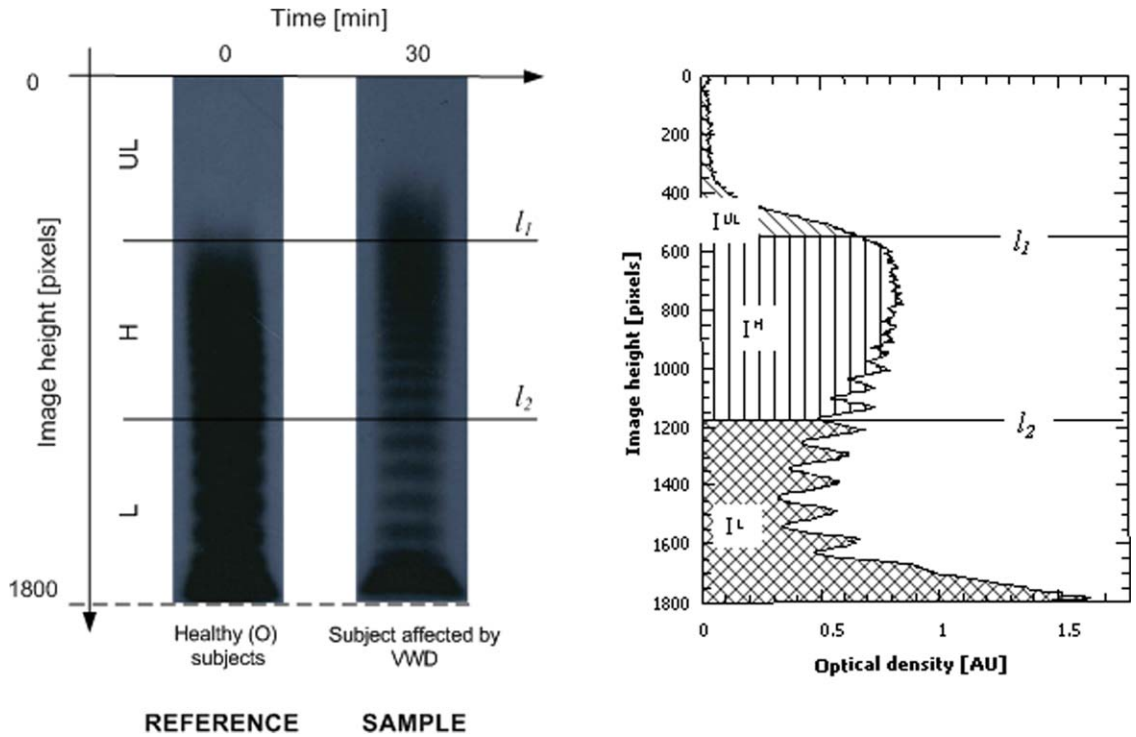

Figure A1. Example of image analysis for a single sample.

(a) Reference lane for a healthy (O) subject and sample for a subject affected by VWD: definition of the UL-H and H-L thresholds; (b) Optical density profile related to the sample as obtained from image analysis.

$$I^{H}=\int_{l_1}^{l_2} Idl \tag{A4}$$

$$I^{L}=\int_{l_2}^{H} Idl \tag{A5}$$

Relations (A4–A6) allow for a semiquantitative definition of the amount of UL, high, and low molecular weight multimers in the sample once the sample mass is known. If the definition of sample weight is not possible or, as it is the case in the present study, it is affected by large uncertainty, the mass fraction z_i of the ith species (UL, H, L) can be calculated from the ratio

$$z_i=I^i/I^{T}=I^i/\sum_i I^i \quad i = \mathrm{UL},\ \mathrm{H},\ \mathrm{L} \tag{A6}$$

where I^{T} is the total area under the curve. The precision on the calculation of the mass fraction is only related to I_i, which is generally less affected to uncertainty than the sample mass.

Manuscript received Oct. 23, 2013, and final revision received Jan. 14, 2014.